

Selective Hydrogenation of Amides using Ruthenium/Molybdenum Catalysts


Graham Beamson,^b Adam J Papworth,^c Charles Philipps,^a Andrew M Smith,^a and Robin Whyman^{a,*}

^a Department of Chemistry, Donnan and Robert Robinson Laboratories, University of Liverpool, Liverpool L69 7ZD, U.K. Fax: (+44)-151-794-3588; phone: (+44)-151-794-3515; e-mail: whyman@liv.ac.uk

^b National Centre for Electron Spectroscopy and Surface Analysis, STFC, Daresbury Laboratory, Warrington, Cheshire WA4 4AD, U.K.

^c Materials Science and Engineering, Department of Engineering, University of Liverpool, Liverpool L69 3GH, U.K.

Received: November 26, 2009; Revised: February 18, 2010; Published online: March 12, 2010

 Supporting information for this article is available on the WWW under <http://dx.doi.org/10.1002/adsc.200900824>.

Abstract: Recyclable, heterogeneous bimetallic ruthenium/molybdenum catalysts, formed *in situ* from triruthenium dodecacarbonyl [Ru₃(CO)₁₂] and molybdenum hexacarbonyl [Mo(CO)₆], are effective for the selective liquid phase hydrogenation of cyclohexylcarboxamide (CyCONH₂) to cyclohexanemethylamine (CyCH₂NH₂), with *no* secondary or tertiary amine by-product formation. Variation of Mo:Ru composition reveals both synergistic and poisoning effects, with the optimum combination of conversion and selectivity at *ca.* 0.5, and total inhibition of catalysis evident at ≥ 1 . Good amide conversions are noted within the reaction condition regimes 20–100 bar hydrogen and 145–160 °C. The order of reactivity of these catalysts towards reduction of different

amide functional groups is primary > tertiary \gg secondary. *In situ* HP-FT-IR spectroscopy confirms that catalyst genesis occurs during an induction period associated with decomposition of the organometallic precursors. *Ex situ* characterisation, using XRD, XPS and EDX-STEM, for active Mo:Ru compositions, has provided evidence for intimately mixed *ca.* 2.5–4 nm particles that contain metallic ruthenium, and molybdenum (in several oxidation states, including zero).

Keywords: amide hydrogenation; heterogeneous bimetallic catalysis; high selectivity; molybdenum; ruthenium

Introduction

The discovery and development of methods for the selective reduction of ‘difficult’ functional groups such as amides, carboxylic acids and esters has been recognised for many years as a formidable problem,^[1] within which grouping amides are acknowledged to represent the most extreme difficulty. The current state of the art requires the use of either expensive reagents, such as LiAlH₄, in *stoichiometric* quantities (with associated environmental clean-up penalties), or traditional copper chromite-based catalysts which, although effective, require very severe reaction conditions, e.g., a minimum of 200 bar H₂ and 250 °C, and high catalyst loadings (*ca.* 20 wt%).^[2] These are clearly unsuitable for the production of intermediates in the manufacture of, for example, pharmaceuticals, which frequently contain multiple sensitive functional

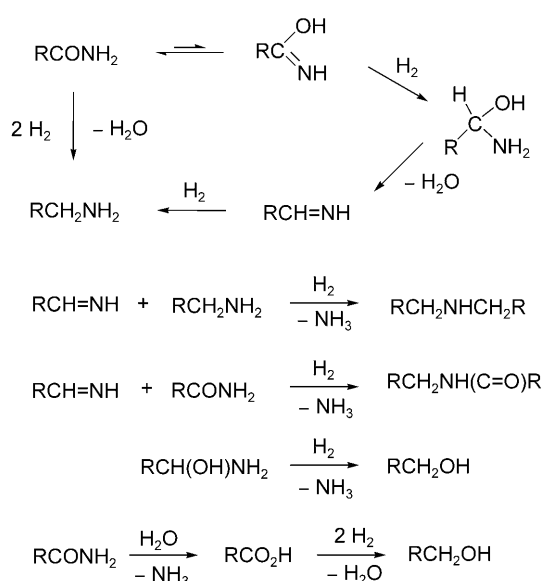
groups. The discovery and development of catalytic methods that are effective under mild reaction conditions, ideally ≤ 30 bar H₂ and 70 °C, represents a challenge that is of particular significance to the fine chemicals industry. Recently a step change in this direction has been provided by reports of a new range of ‘bimetallic’ catalysts, particularly those derived from organometallic precursors such as Rh and Mo carbonyls, initially described as homogeneous,^[3–5] and typically exemplified by the reduction of the tertiary amide *N*-acetylpiperidine to *N*-ethylpiperidine at 100 bar H₂ and 160 °C.^[4] We have described details of the genesis and characterisation of such catalysts, formed *in situ* from Rh₆(CO)₁₆ and Mo(CO)₆, and unequivocally demonstrated that they are in fact heterogeneous.^[6] Their performance in the selective hydrogenation of a representative primary amide such as cyclohexylcarboxamide to the corresponding primary

amine, cyclohexanemethylamine [(Eq. (1)) in up to 87% selectivity, was found to be critically dependent on the Mo:Ru composition. The only by-products de-



Cy = *c*-C₆H₁₁

tected in significant amounts were the secondary amine *N*-(cyclohexylmethyl)-cyclohexanemethanamine, (CyCH₂)₂NH and cyclohexanemethanol, CyCH₂OH (*cf.* proposed reaction pathways, summarised in Scheme 1), together with traces (typically <1%) of methylcyclohexane.



Scheme 1. Primary amide hydrogenation: reaction pathways to by-products, highlighting the significance of the postulated imine intermediate. † There is a paucity of information concerning mechanistic reaction steps involved in amide hydrogenation. Although there is no direct evidence for the involvement of imine intermediates their transient presence does conveniently account for secondary and tertiary amine by-product formation in the reduction of amides (and nitriles).

Bimetallic Ru-containing catalysts are well established for carbonyl group reduction, see for example,^[7,8] and ruthenium should therefore also represent a strong candidate for amide hydrogenation, a view that is reinforced by the knowledge that Ru is also an effective catalyst for the selective reduction of nitriles to amines.^[9] Here we report the genesis of a family of Ru/Mo catalysts, prepared *in situ* in an analogous manner to the Rh/Mo systems, and their performance in the reduction of a representative selection of primary, secondary and tertiary amides. An analogous terminology to that used in the Rh/Mo work has been employed, namely Ru/Mo, except where reference has been made to variations in Ru/Mo content and where the reciprocal terminology Mo:Ru most effectively highlights the very significant effects resulting from addition of minor quantities of Mo to poorly performing Ru catalysts.

Results and Discussion

CyCONH₂ Hydrogenation using Ru/Mo Catalysts

The results of preliminary experiments with CyCONH₂ using various Ru catalyst precursors, and two to which Mo(CO)₆ have been added, are summarised in Table 1.

With Ru alone (entries 1 and 2) *no* primary amine was formed, and the product distribution approximated to a 2:1 mixture of CyCH₂OH and (CyCH₂)₂NH at similar CyCONH₂ conversion levels of *ca.* 35%. The co-addition of Mo(CO)₆ at an Mo:Ru atomic ratio of 0.50 (entry 3) resulted in a profound effect on catalytic behaviour, with both considerably improved amide conversion but far more importantly product selectivity, namely a complete switch in product distribution to a *ca.* 6:1 mixture of the desired primary amine CyCH₂NH₂ and CyCH₂OH, with total *absence* of secondary amine formation, thus representing a highly unusual feature of amide reduction chemistry.^[2] In contrast, reference Ru/MoO₃ and Ru/Mo powder catalysts prepared using Ru₃(CO)₁₂ (entries 5 and 6) both showed behaviour that was typical of Ru alone.

Table 1. CyCONH₂ hydrogenation: conversion and product selectivity using bimetallic Ru/Mo and Ru catalyst precursors.^[a]

Entry	Catalyst precursor	Conversion [%]	Product Selectivity [%]		
			CyCH ₂ NH ₂	CyCH ₂ OH	(CyCH ₂) ₂ NH
1	Ru ₃ (CO) ₁₂	35	0	62	36
2	Ru/C	32	0	68	31
3	Ru ₃ (CO) ₁₂ /Mo(CO) ₆	100	85	14	0
4	Ru(acac) ₃ /Mo(CO) ₆	100	85	10	4
5	Ru ₃ (CO) ₁₂ /MoO ₃	35	0	66	29
6	Ru ₃ (CO) ₁₂ /Mo powder	36	0	64	33

^[a] Catalyst concentration: 5 mol% Ru; Mo:Ru = 0.50; reaction conditions: 100 bar H₂, 160 °C, 16 h.

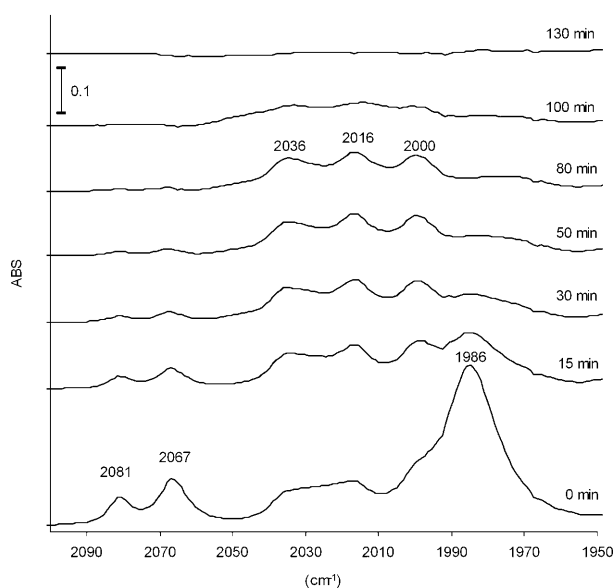


Figure 1. *In situ* HP-FT-IR spectra (2100–1950 cm^{-1}) during catalyst genesis using $\text{Ru}_3(\text{CO})_{12}/\text{Mo}(\text{CO})_6$ in DME at 100 bar H_2 , 160 °C.

In situ HP-FT-IR spectroscopy (in the range 2100–1950 cm^{-1}) was used to monitor changes that occurred as a function of time using the catalyst composition corresponding to Table 1, entry 3. Figure 1 shows that loss of all Ru/Mo metal $\nu(\text{CO})$ absorptions was complete after the first 130 min of reaction at 160 °C. CyCONH_2 reduction was initiated after this induction period, as shown by the decay profile of the amide carbonyl absorption at 1693 cm^{-1} (Figure 2). Analysis of this curve, using the first four points from the end of the induction period, i.e., over the time period 100–170 min, gave an estimated initial TON (mmol CyCONH_2 consumed *vs.* mmol Ru) of 4.7 h^{-1} . After reaction at 100 bar H_2 and 160 °C for 16 h the product solutions appeared colloidal [see Supporting Information, Figure S1 (b)]. Settlement occurred slowly on standing, with the deposition of black residues, leaving a clear supernatant product solution [see Supporting Information, Figure S1 (c)], suggesting that the real catalysts were heterogeneous. Analysis of spectroscopic changes occurring during the initiation period, together with results of control experiments using, e.g., $\text{Ru}_3(\text{CO})_{12}$ alone, have enabled the assembly of a complete picture of the molecular species present in solution during catalyst genesis (see below).

Variation of Mo:Ru Composition

Figure 3 shows the effects, on conversion and product selectivity, of variation of Mo:Ru, from which it is evi-

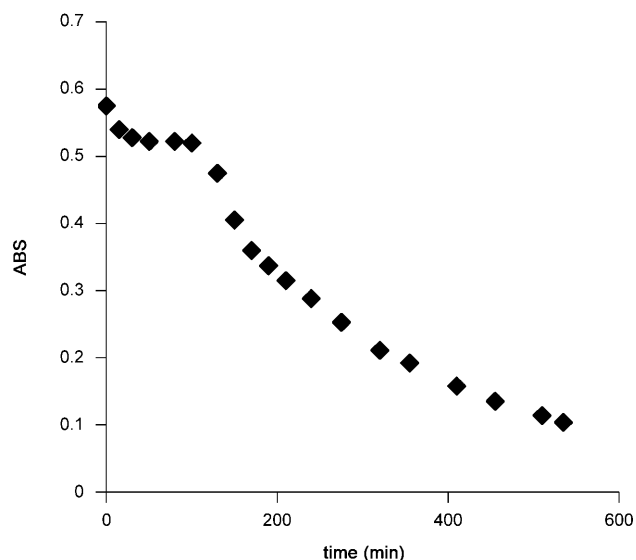


Figure 2. CyCONH_2 hydrogenation: decay profile of 1693 cm^{-1} amide carbonyl absorption band monitored by HP-FT-IR using an Mo:Ru=0.50 catalyst at 100 bar H_2 and 160 °C.

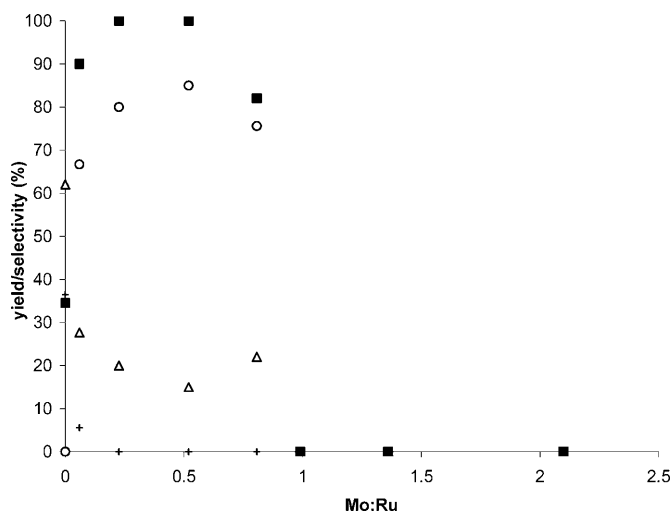


Figure 3. CyCONH_2 hydrogenation: conversion and product selectivity *vs.* variation in Mo:Ru catalyst composition (100 bar H_2 , 160 °C and 16 h). Key: ■ conversion, ○ $\text{CyCH}_2\text{NH}_2 + (\text{CyCH}_2)_2\text{NH}$, △ CyCH_2OH .

dent that only very minor quantities of $\text{Mo}(\text{CO})_6$ (e.g., Mo:Ru=0.06) were necessary to initiate synergistic effects. The optimum combination of amide conversion and primary amine selectivity (typically 85% CyCH_2NH_2 and 14% CyCH_2OH) was found with Mo:Ru values of *ca.* 0.5; furthermore, complete catalyst deactivation was evident at Mo:Ru ≥ 1 . With increasing Mo content over the composition range Mo:Ru=0–0.5 selectivity towards the primary amine increased as that towards CyCH_2OH decreased, with

the converse applying over the range Mo:Ru=0.5–0.8. Significant secondary amine formation (36% selectivity at 35% conversion) was only evident in the absence of Mo.

Variation of Pressure and Temperature

The effects of pressure and temperature variations on CyCONH₂ reduction, using the optimum Mo:Ru=0.50 catalyst precursor, are summarised in Table 2, from which it is clear that primary amine selectivity was essentially independent of hydrogen pressure over the range 100–10 bar; moreover a significant decrease in conversion was only detected between 20 and 10 bar (entries 1–4). In contrast, conversions appeared extremely temperature dependent, showing a very marked decline between 145 and 140 °C (*cf.* entries 1, 5–7), also accompanied by a minor decrease of primary amine selectivity, and zero conversion at 130 °C. These temperatures represent a limiting requirement for reactions in which the catalyst is formed *in situ*. It is noteworthy that no secondary amine was formed at 100 bar H₂ throughout the temperature range 160–140 °C, although traces were detected at 50 bar H₂ and below. Temperature would be expected to exert a significant influence on the length of the induction period required for full decomposition of the metal carbonyl precursors, with lower temperatures likely to necessitate longer times. Thus, slower/incomplete decomposition might account for the reduced conversions noted at lower temperatures. This limitation should not necessarily apply to pre-formed catalysts, although even here (entries 8 and 9) it is quite evident that conversions were substantially reduced at lower temperatures, notwithstanding considerably extended reaction times. Reaction condition combinations of either 20 bar H₂/160 °C or 100 bar H₂/145 °C appear to be the lower limiting operating parameters for reduction of CyCONH₂.

The explanation for the limiting temperature dependence on conversion seems most likely to be related to the balance between the adsorption/desorption behaviour of reactants and products. In this respect amide adsorption would be expected to be more sensitive than amine desorption. Amide adsorption would become less favoured with increasing temperature, whereas amine desorption should be less sensitive and possibly largely independent of temperature. It is therefore possible that, at temperatures below the threshold for catalytic reduction, the amide substrate is simply too strongly chemisorbed on the Ru/Mo surface. Such temperature limitations will be sensitive to the intimate nature of the catalyst and, for example, the recently reported Rh/Mo catalysts exhibited high CyCONH₂ conversions at 130 °C (and 100 bar H₂) but with significantly reduced primary amine selectivity (53%), and both (CyCH₂)₂NH (23%) and CyCH₂OH (19%) formation.^[6]

Additional Reaction Variables

The results of variation of other reaction parameters such as solvent, exposure of the systems to CO and air, and attempted *in situ* removal of water during Ru/Mo-catalysed CyCONH₂ reduction, are detailed in the Supporting Information S1.

Catalyst Separation and Recycle

After all ‘single-pot’ reactions, complete settlement of the fine particulates from DME solution could require an extended period of time (see Supporting Information, Figure S1) and this might account for earlier suggestions that these were homogeneous catalysts.^[3–5] Nevertheless, used catalysts required no further treatment, other than separation and washing, and could be readily recycled under the standard

Table 2. CyCONH₂ hydrogenation: conversion and product selectivity vs. pressure and temperature (Mo:Ru=0.50 catalyst).

Entry	T [°C]	P _{H₂} [bar]	Conversion [%]	Product Selectivity [%]		
				CyCH ₂ NH ₂	CyCH ₂ OH	(CyCH ₂) ₂ NH
1	160	100	100	85	14	0
2	160	50	99	84	12	3
3	160	20	97	85	13	2
4	160	10	63	87	11	1
5	150	100	100	83	16	0
6	145	100	99	83	17	0
7	140	100	44	80	20	0
8	130 ^[a]	100	70	77	23	0
9	120 ^[b]	100	10	major product	–	–

^[a] Using pre-formed catalyst; reaction time: 68 h.

^[b] Using pre-formed catalyst; reaction time: 96 h.

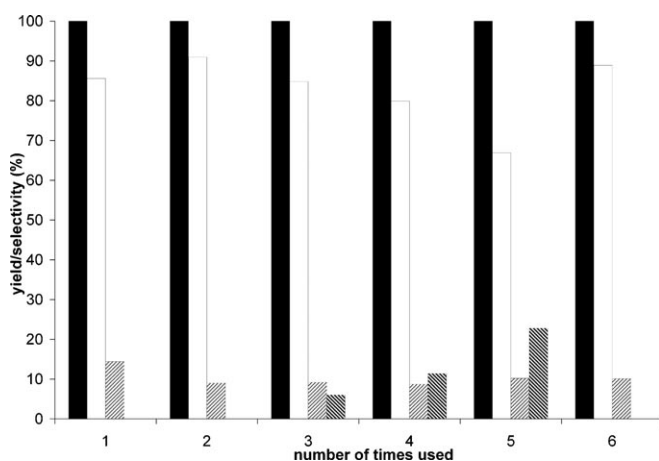


Figure 4. CyCONH₂ hydrogenation: product selectivity vs. recycle using a Mo:Ru=0.57 catalyst. Key: ■ conversion, □ CyCH₂NH₂, ▒ CyCH₂OH, ▓ (CyCH₂)₂NH. Cycle 6 with addition of LiOH.

processing conditions. The behaviour of a representative optimum catalyst (Mo:Ru=0.57) towards recycle is indicated in Figure 4.

Complete amide conversions are evident throughout and CyCH₂OH formation remains essentially constant, although primary amine selectivity decreases slightly during cycles 3–5, in which the first appearance and increase in secondary amine formation is evident. This variation in selectivity seems most likely to be a consequence of sequential retention and accumulation of minor amounts of insoluble C-, H-, and N-containing residues on the catalyst surface. Such material would be resistant to removal during catalyst separation and centrifugation and may lead to more prolonged residence times of reactants and intermediates on the catalyst surface, thus favouring condensation reactions with the postulated imine intermediate (cf. Scheme 1), and a resultant increase in (CyCH₂)₂NH production, as observed. However, addition of trace quantities of a strong base in the form of LiOH·H₂O (1 mg), in accordance with a literature precedent for the hydrogenation of nitriles,^[10] prior to cycle 6 resulted in complete suppression of secondary amine formation, and restoration of the initial primary amine selectivity to 90% (cf. cycle 2). The role of LiOH addition has previously been attributed to favouring rapid desorption of the amine, thus leading to inhibition of side reactions.^[9]

Variation of Amide Substrates

The behaviour of the optimum (Mo:Ru=0.50) catalyst composition for CyCONH₂ reduction towards a representative selection of aliphatic, cyclo-aliphatic and aromatic primary, secondary and tertiary amide substrates, including in particular, close derivatives of

cyclohexanecarboxamide, was evaluated and the results are summarised in Table 3. These substantiate the general applicability of Ru/Mo catalysts towards amide reduction and provide a qualitative evaluation of the relative ease of hydrogenation in the order primary > tertiary > secondary.

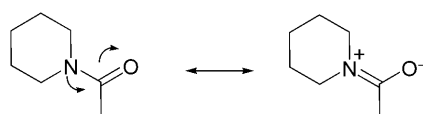
Amongst primary amides, benzamide (Table 3, entry 1), the aromatic analogue of CyCONH₂, which should be more activated towards reduction because of the electron-withdrawing nature of the aromatic ring, did indeed display extremely similar behaviour in respect of both conversion and selectivity (cf. Table 1, entry 3). This is presumably a reflection and confirmation that, here at least, hydrogenation of the aromatic ring is facile in relation to the far more demanding nature of amide functional group reduction, and there is thus no suggestion of catalyst inhibition by the presence of the aromatic ring (see below). The aliphatic primary amide *n*-butyramide (Table 3, entry 2) afforded *n*-butylamine in high selectivity with no detectable secondary amine formation, whereas the more sterically hindered trimethylacetamide (entry 3) yielded predominantly 2,2-dimethylpropan-1-ol and only 40% selectivity towards the expected product, 2,2-dimethylpropanamine. The secondary amides *N*-methylbenzamide (entry 4) and *N*-methylcyclohexanecarboxamide (entry 5) proved significantly more resistant to reduction. Although the aromatic ring was readily reduced, only minor overall conversions to the secondary amine were evident. Reaction of the secondary amide *N*-methylformamide, HCONHCH₃, was also followed by *in situ* HP-FT-IR spectroscopy. Some reduction was evident from a significant decrease in intensity of the ν(CO) amide absorption at 1694 cm⁻¹, but it proved impractical to quantify the product distribution by GC analysis because of the high volatility of the principal reaction product, dimethylamine, detected by its odour in the off-gases during depressurisation. Tertiary amides (Table 3, entries 6–9) were more readily reduced than secondary amides (cf. entries 4 and 5), although with wider variation in product selectivity. *N,N*-Dimethylbenzamide (entry 6) showed similar behaviour to that of benzamide (entry 1) in terms of preferred aromatic ring reduction, but the high residual CyCON(CH₃)₂ content and only 30% overall conversion to CyCH₂N(CH₃)₂ suggested significant catalyst inhibition. Nevertheless, a similar 30% overall amide to amine conversion was evident with *N,N*-dimethylcyclohexanecarboxamide (entry 7). *N,N*-Diethylpropionamide (entry 8), an example of a conventional aliphatic tertiary amide, yielded *N,N*-diethylpropylamine as the major product. *N*-Acetylpiperidine (NAP; entry 9) underwent complete conversion to *N*-ethylpiperidine in 90% selectivity, behaviour which is very similar to that observed with Rh/Mo catalysts.^[6] Although used as a standard substrate by Fuchikami et al.,^[4] it is im-

Table 3. Products of amide hydrogenation (Mo:Ru = 0.50 catalyst).^[a]

Entry	Substrate	Conversion [%]	Products	Selectivity [%]
1		100	CyCH ₂ NH ₂ /CyCH ₂ OH	83/16
2		100	<i>n</i> -butylamine/no (C ₄ H ₉) ₂ NH/ <i>n</i> -butanol	77/22
3		100	2,2-dimethylpropanamine/2,2-dimethylpropan-1-ol	40/60
4		100 ^[b]	CyCH ₂ NHCH ₃ /CyCONHCH ₃	8/85
5		5	CyCH ₂ NHCH ₃ (traces)	
6		100 ^[b]	CyCH ₂ N(CH ₃) ₂ /CyCH ₂ OH/CyCON(CH ₃) ₂	30/5/65
7		30	CyCH ₂ N(CH ₃) ₂ /CyCH ₂ OH	73/27
8		100	C ₃ H ₇ N(C ₂ H ₅) ₂ (major product)	
9		100	<i>N</i> -ethylpiperidine/piperidine	90/10

^[a] Reaction conditions: 100 bar H₂, 160 °C, 16 h.^[b] NB: 100% aromatic ring reduction, but considerable unreacted saturated amide.

portant to recognise that NAP (and *N*-acetylpyrrolidine), whilst providing convenient model amides in terms of availability and limited number of potential reduction products, are not representative of typical tertiary amide structures because the amide N-atoms are integral components of six (and five)-membered rings.^[6] Amide reduction may be facilitated by the formation of ring-stabilised zwitterions (*cf.* Scheme 2), with the charge separation between O and N atoms resulting in stronger C–N bonds, and correspondingly

**Scheme 2.** Neutral and zwitterionic forms of *N*-acetylpiperidine.

weaker C–O bonds, thus assisting addition of H₂ in a manner that is less accessible to more typical tertiary amides.

A possible explanation for the observed order of reactivity primary > tertiary ≫ secondary amide is that the greater degree of steric hindrance presented by *N*-methyl substituents acts to hinder adsorption. In simplistic terms tertiary amides would be expected to present even greater resistance to reduction but an additional important factor for consideration is the respective orientation of each amide on the catalyst surface. An alternative explanation for the apparent resistance of secondary amides to reduction concerns stabilisation as a consequence of their propensity to form exceptionally strongly hydrogen-bonded dimers in solution, as exemplified in peptide chemistry,^[11] although this does perhaps seem unlikely to be dominant at the temperatures used during catalysis. The

above ordering of reactivity parallels the trend noted using standard *stoichiometric* hydride reduction methods with, for example, LiAlH_4 .^[12] Reports of the use of the less aggressive reducing agent NaBH_4 towards reduction of amides at high temperatures^[13,14] are also instructive. Here, secondary amides are unreactive, tertiary amides give the corresponding amine in moderate yield, whereas primary amides undergo initial dehydration to the nitrile followed by slow reduction to the amine, a point that may be of significance in mechanistic terms. Ru catalysts are well known to be effective for selective reduction of nitriles to primary amines,^[9] and such a demonstration of an amide dehydration step to the nitrile could conceivably provide an initial mechanistic pathway of lower energy that is accessible only to primary amides. The operation of such a pathway might also explain the switch in product distribution with 2,2-dimethylpropionamide (Table 3, entry 3) where dehydration to the nitrile might be expected to be more difficult than with *n*-butyramide.

Controlled Addition of Water

Since water is a primary product of amide hydrogenation [Eq. (1)], and at the end of these reactions should therefore be present in equivalent amounts to the amine(s) formed, it was appropriate to determine whether the presence of additional water at the outset would be beneficial, or otherwise, to reaction rate and selectivity. It is also relevant to note that small amounts of water are commonly recognised to act as promoters of many chemical processes, e.g., nitrile hydrogenation over unsupported Co catalysts, where the addition of H_2O leads to enhanced yields of primary amine.^[9] Table 4, entries 2 and 3, show the effects of the addition of 1 and 5 equivalents of water (relative to amide) to a Mo:Ru=0.50 catalyst at the start of the reaction, clearly highlighting the incremental reduction in selectivity to primary amine in favour of CyCH_2OH . In a further experiment, Table 4, entry 4, in which D_2O was used for putative labelling studies, the addition of 30 equivalents of D_2O resulted not only in a drastic reduction in conversion but also a complete switch of selectivity in favour of

$\text{CyCH}_2\text{O}(\text{H/D})$, but still without any secondary amine formation.

Reference to the proposed reaction pathways for amide reduction (Scheme 1) suggests that CyCH_2OH formation may occur *via* competitive hydrogenolysis of the intermediate aminocarbonol with the loss of ammonia (hence the reasoning for the conventional addition of NH_3 to suppress secondary amine formation). Since water is released during conversion of aminocarbonol to the postulated imine, accumulation of additional water would presumably serve to inhibit this step, leading to a higher standing aminocarbonol concentration, thereby favouring CyCH_2OH formation. Although it appears rather unlikely at very low water levels, an alternative potential competing reaction pathway that requires consideration is initial, rather demanding^[12] hydrolysis of CyCONH_2 to cyclohexanecarboxylic acid, followed by reduction. Using the optimum Mo:Ru catalyst composition (0.50) and standard reaction conditions (100 bar H_2 , 160 °C, 16 h), CyCO_2H underwent 85% conversion (*cf.* complete reduction of CyCONH_2 , Table 1) to CyCH_2OH and methylcyclohexane (in 75 and 18% selectivity, respectively), with additional traces of coupled products. This demonstrates not only the viability of Ru/Mo catalysts in the second step of a potential alternative pathway from CyCONH_2 to CyCH_2OH , but also an indication of their applicability towards reduction of carboxylic acids in general.

Catalyst Genesis using HP-FT-IR Spectroscopy

In situ studies of the complete Ru/Mo precursor catalyst system (Figure 1), together with control experiments using Ru and Mo carbonyls, e.g., $\text{Ru}_3(\text{CO})_{12}$ in DME alone, have enabled a full description of the molecular transformations involved during catalyst evolution.

For Ru alone, spectroscopic changes occurring during slow incremental heating over the range 25–160 °C (Figure 5) are consistent with the initial transformation of $\text{Ru}_3(\text{CO})_{12}$ into $\text{H}_4\text{Ru}_4(\text{CO})_{12}$ in accordance with literature precedent [Eq. (2)].^[15]

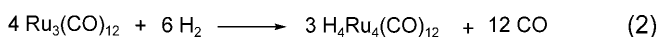


Table 4. CyCONH_2 hydrogenation: conversion and product selectivity vs. incremental addition of water (Mo:Ru=0.50 catalyst).

Entry	$\text{H}_2\text{O}/\text{D}_2\text{O}$	Conversion [%]	Product selectivity [%]	
			CyCH_2NH_2	CyCH_2OH
1	none	100	85	14
2	H_2O (1 equiv.)	100	82	16
3	H_2O (5 equiv.)	100	77	22
4	D_2O (30 equiv.)	30	26	74

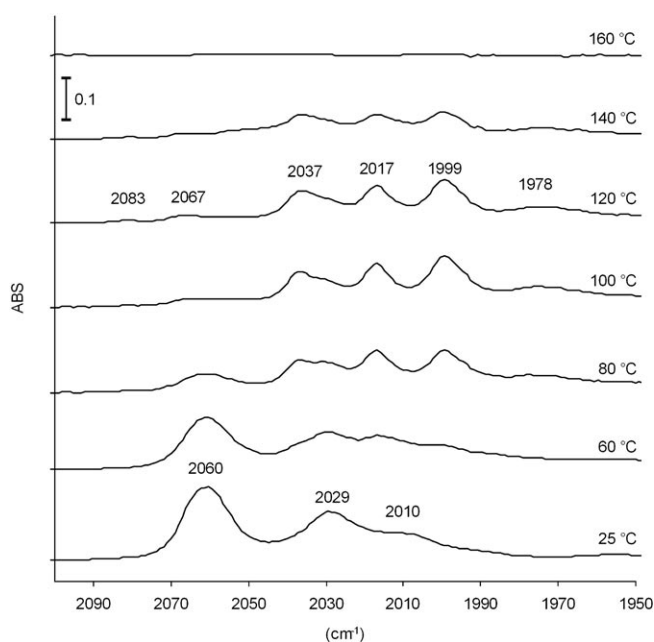
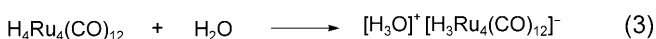


Figure 5. *In situ* HP-FT-IR spectra (2150–1950 cm^{−1}) showing the transformations of Ru₃(CO)₁₂ in DME at 100 bar H₂ and 25–160 °C.

Further reaction occurs at 100 °C with the formation of [H₃Ru₄(CO)₁₂][−]^[16] an anion that has been reported to be a deprotonation product of H₄Ru₄(CO)₁₂ in methanol^[17] and, because of the absence of Mo(CO)₆ [with intense ν(CO) at 1986 cm^{−1}, *cf.* Figure 1], the additional characteristic absorption of this anion at 1978 cm^{−1} is also clearly visible (for band frequencies see Supporting Information Table S1). The driving force for transformation from neutral to anionic Ru seems likely to comprise reaction with water [Eq. (3)] formed by methanation of the CO re-



leased according to Eq. (2). Evidence in support of water formation has been provided by the appearance and growth of ν(O–H) absorption bands at 3590 and 3518 cm^{−1}.

Traces of H₄Ru₄(CO)₁₂ are identifiable up to 140 °C, a further increase in temperature to 160 °C resulting in complete disappearance of all ν(CO) absorptions.

In the full Ru/Mo catalyst system (Figure 1) the spectrum initially recorded after rapid heating to 160 °C (at 0 min) corresponds to a mixture of H₄Ru₄(CO)₁₂ and Mo(CO)₆. The intense absorption at 1986 cm^{−1} due to the latter disappears after 30 min, leaving [H₃Ru₄(CO)₁₂][−] in solution, which survives for over 100 min (i.e., approaching the length of the observed induction period). However, in the initial

stages, the anion appears to catalyse the rapid decomposition of Mo(CO)₆ at 160 °C (Figure 1), the 1986 cm^{−1} absorption decreasing in intensity and disappearing completely after *ca.* 30 min. This behaviour is in marked contrast to the extended stability (in excess of 16 h) of Mo(CO)₆ in DME alone under the same reaction conditions.^[6] It appears therefore that Mo(CO)₆ may provide a convenient source of CO that is scavenged by Ru to sustain the stability of [H₃Ru₄(CO)₁₂][−] during the catalyst induction period. A precedent for this suggestion is available from the demonstration of a similar, but reversible, reaction in which ionic Ru and neutral Ir carbonyl intermediates exchange CO in the proposed mechanism for Ir-catalysed methanol carbonylation in the presence of Ru promoters.^[18] It is also relevant to note that the bond enthalpy of the Mo–C bond in Mo(CO)₆ (151 kJ mol^{−1})^[19] is lower than that of the Ru–C bond (164 kJ mol^{−1}) in Ru₃(CO)₁₂.^[20]

Once the available CO from Mo(CO)₆ has been consumed, [H₃Ru₄(CO)₁₂][−] itself slowly degrades, total loss of ν(CO) absorptions coinciding with the onset of catalytic activity. Although no supporting spectroscopic evidence has been obtained for the presence of mixed Ru–Mo carbonyl species in solution (it is significant to note that no equivalent binary carbonyls have been reported in the literature, and the few examples of mixed Ru–Mo complexes that are known contain either cyclopentadienyl or tertiary phosphine ligands), the accelerated decomposition of Mo(CO)₆ in the presence of Ru carbonyl seems indicative of an intimate association between the two elemental components during controlled catalyst genesis.

In addition to the Ru and Mo carbonyl components, the nature of the amide substrates themselves appears to exert an influence on the catalyst activation process, as variations in the length of induction period with different amides bear witness. In contrast to the *ca.* 2 h required by CyCONH₂, induction periods of 6 and greater than 8 h, respectively, were evident with the secondary amides CyCONHCH₃ and HCONHCH₃; throughout which the presence of [H₃Ru₄(CO)₁₂][−] was retained. There is ample precedence for the formation of amide-substituted metal carbonyls, particularly with Mo,^[21] although the situation with respect to Ru is less clear. Both the stoichiometry and stability of such products are likely to be dictated by the nature of the individual amide, which can therefore reasonably be expected to lead to variations in the degree of inhibition towards complete decomposition. Hence the most likely explanation for the variation in length of the induction periods is an amide-dependent stabilisation of Mo(CO)_{6−x}(amide)_x (x = 1–3),^[21] which in turn limits the rate of total decomposition at 160 °C and allows the controlled assembly of the respective Ru/Mo catalysts.

Ex situ Catalyst Characterisation

XRD profiles and parameters, including mean crystallite sizes (estimated using the Scherrer equation applied to the most intense (101) Ru Bragg reflection at $2\theta = ca. 51.5^\circ$), of materials containing a range of Mo:Ru values are shown in Figure 6 and Table 5, respectively. Dominant features of the profiles are consistent with the diffraction pattern expected for hexagonal Ru with no evidence of any discrete crystalline Mo-containing phase(s). Broad profiles are observed for the bimetallic Ru/Mo samples, indicative of either small particle sizes and/or low crystallinity. For that with the lowest nominal Mo content, Mo:Ru=0.52, representative of the most active and selective catalyst for CyCONH₂ reduction (Table 5, entry 2), the profile is particularly broad, equating to a mean Ru crystallite size of *ca.* 2.6 nm. The catalytically inactive materials, with successively higher Mo:Ru ratios (entries 3 and 4), contain larger (6–7 nm) aggregates which are nevertheless still smaller than the value of 8.2 nm obtained from the reference Ru sample prepared from the reaction of Ru₃(CO)₁₂ alone (entry 1). Calcination of the Mo:Ru=0.52 catalyst at 300 °C for

3 h results in a considerably sharper XRD profile (Figure 6) with parameters (Table 5, entry 5) that correspond closely with the reference values for bulk metallic Ru,^[22] thus reflecting the extensive sintering that occurs during treatment at considerably higher temperatures than the maximum of 160 °C used for catalytic amide reduction. Comments on additional minor features of XRD data are included in the Supporting Information, S2.

The optimum Ru/Mo (Mo:Ru=0.50) amide reduction catalyst and reference material Ru/MoO₃ [ex-Ru₃(CO)₁₂] (Mo:Ru=0.53), were examined by EDX-STEM microscopy. Nine different areas of the former, all of which exhibited closely similar features, were mapped by STEM and analysed. Figure 7 illustrates, in high magnification, the bright field image of one typical area, examination of which reveals several agglomerates in the size range 30–50 nm; localised within these agglomerates, smaller areas (*ca.* 2.5–4 nm, *cf.* XRD data, Table 5) of higher contrast are apparent. Individual Mo and Ru L maps are shown in

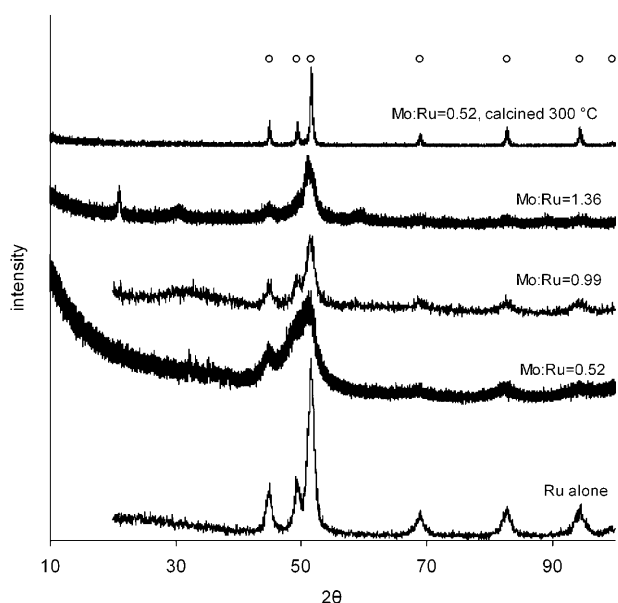


Figure 6. XRD profiles of Ru/Mo catalysts. ° Parameters for metallic Ru.^[22]

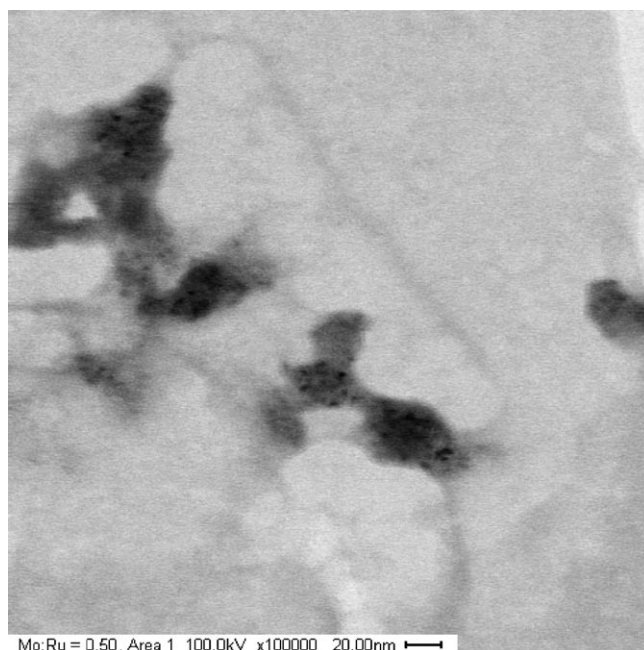


Figure 7. EDX-STEM analysis: bright field image of typical area of Mo:Ru=0.50 catalyst.

Table 5. XRD data: 2θ values, d -spacings and mean particle sizes of Ru:Mo catalysts.

Entry	Sample	Ru (101) 2θ value [°]	d -spacing [Å]	Mean crystallite size [nm]
1	Ru	51.56	2.058	8.2
2	Mo:Ru=0.52	51.36	2.066	2.6
3	Mo:Ru=0.99	51.36	2.066	6.4
4	Mo:Ru=1.36	51.26	2.069	6.9
5	Mo:Ru=0.52 calcined 300 °C	51.65	2.055	26.5
6	Ru reference ^[22]	51.62	2.056	–

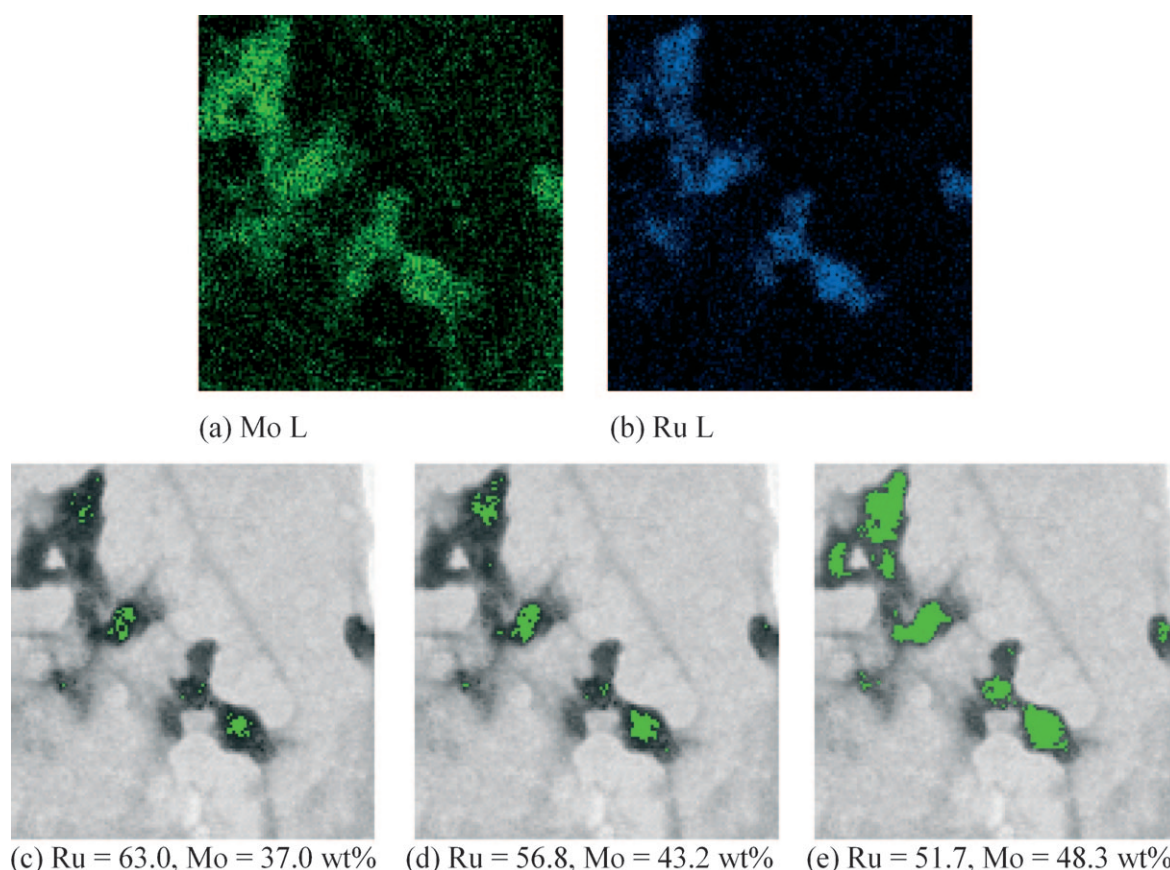


Figure 8. EDX-STEM analysis of Mo:Ru=0.50 catalyst: (a) Ru L(2.559 keV) and (b) Mo L(2.293 keV) maps, (c–e) Ru, Mo quantification, areas of analysis depicted in light green.

Figure 8 (a) and (b), their comparison showing clearly that wherever Ru is detected Mo is also present, thus confirming a close association between Ru and Mo; Mo alone is also evident, in lower concentrations, distributed across other areas of the sample. Quantification of the constituent elements, selected by particle density, over areas of the micrograph highlighted in green, Figure 8 (c)–(e), show a progressive increase in Mo content, from 37% in the small areas of highest contrast (c) to *ca.* 50% over the larger, broader areas of lower contrast (d), (e). These materials of *ca.* 2.4–4 nm diameter appear extremely well intermixed and homogeneous in composition. In complete contrast, Figure 9 reveals that the reference Ru/MoO₃ [ex-Ru₃(CO)₁₂] sample, which exhibited typical behaviour of a standard supported Ru catalyst, e.g., Ru/C (Table 1, entries 2 and 5) towards CyCONH₂ reduction, contains discrete Ru particles of mean diameter 8 nm (*cf.* Table 5, entry 1) distributed around the edges of platelets of MoO₃, with very clear segregation between Ru and Mo components.

Close inspection of the XRD parameters of three samples with successively higher nominal Mo to Ru ratios (Table 5, entries 2–4) reveals a consistent slight increase in *d*-spacing relative to metallic Ru (entry 5). The origin of this hcp Ru lattice expansion may be

tentatively associated with some substitution by Mo. Ruban et al.^[23] have reported surface segregation energies for binary combinations of the transition metals. The Ru lattice is considered to be a poor host for most second row metals where either ‘strong, or very strong, segregation’ predominates. However, an exception is noted when Mo comprises the solute and here ‘moderate antisegregation’ is said to occur, with positive surface segregation energies $E_{\text{seg}}=0.05\text{--}0.3$ eV. Calcination and sintering of the Mo:Ru=0.52 sample at 300 °C presumably results in expulsion of any postulated interstitial Mo from the Ru lattice (*cf.* Table 5, entry 5).

XPS data were recorded for three Ru/Mo catalysts [Mo:Ru=0.19, 0.57 (recycled) and 1.51], and the reference material, Ru/MoO₃ [ex-Ru₃(CO)₁₂] (Mo:Ru=0.53). All exhibited a dominant Ru 3d_{5/2} line at *ca.* 280.1 eV (which sharpened slightly on Ar⁺ sputter etching), consistent with the metallic Ru(0) state. Mo 3d spectra were considerably more complex, with several different Mo environments evident in all examples examined. A particularly clear profile for the catalytically active and selective Mo:Ru=0.19 composition (*cf.* Figure 3) is shown in Figure 10.

Use of curve fitting techniques reveals the presence of four distinct components with 3d_{5/2} lines centred at

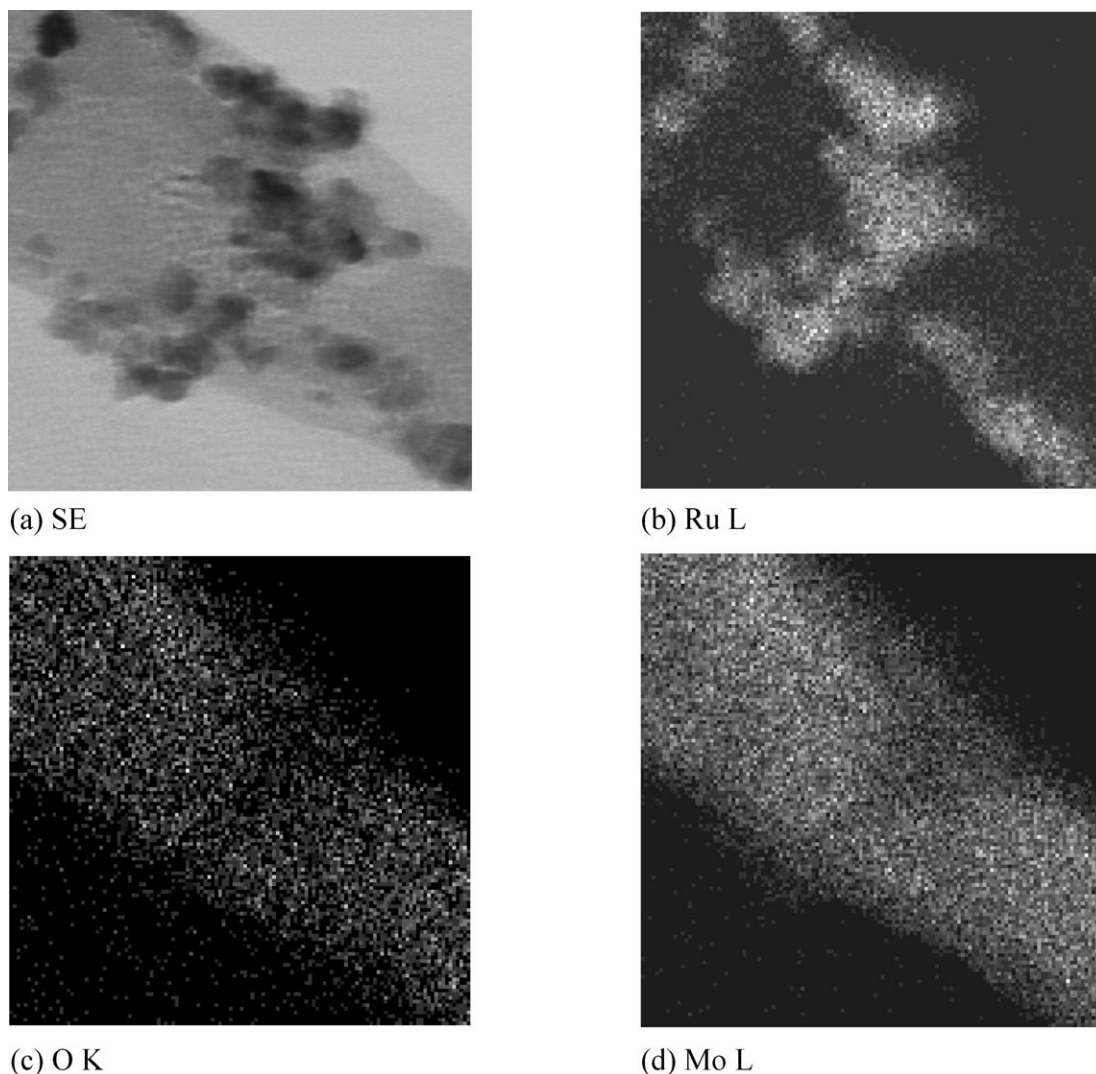


Figure 9. EDX-STEM analysis: (a) bright field image, (b) Ru (L), (c) O (K) and (d) Mo (L), maps of Ru/MoO₃ [ex-Ru₃(CO)₁₂], Mo:Ru=0.53.

232.4, 231.3, 228.7 and 228.0 eV, and which, by comparison with known standards^[6] may be assigned to Mo(VI), Mo(V), Mo(IV) and, most notably *zerovalent* Mo environments, respectively. Significant, but different, amounts of each of these states were detected in all the Ru/Mo catalysts derived from both metal carbonyls. In contrast, XPS spectra of the Ru/MoO₃ [ex-Ru₃(CO)₁₂] sample revealed a much simpler Mo 3d_{5/2} profile (Figure 11), with Mo(VI) (62.2%) and Mo(IV) (29.3%) as major components, a minor amount of Mo(V) (8.5%), and most significantly, *no* zerovalent Mo.

In the as-prepared state the Mo(VI), Mo(V), Mo(IV) and Mo(0) distribution for the Mo:Ru=0.19 catalyst comprises 52, 24, 11, and 13 at%, respectively (Table 6), reference to which shows that the surface concentration of Mo decreases slightly, with a concomitant increase in Ru, following Ar⁺ sputter etching. The concentration of Mo(VI), as a fraction of

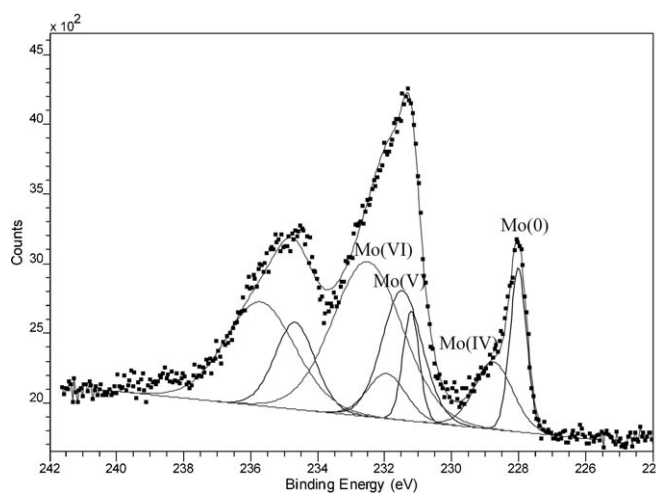


Figure 10. XPS data: curve fitting of Mo 3d region of Mo:Ru=0.19 catalyst.

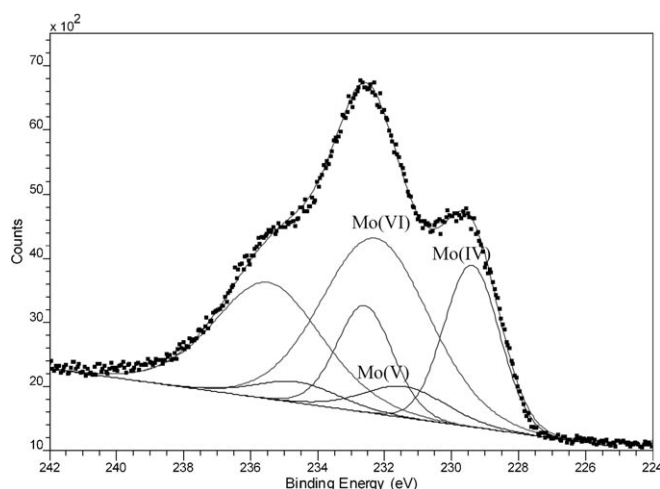


Figure 11. XPS data: curve fitting of Mo 3d region of Ru/MoO₃ [ex-Ru₃(CO)₁₂], Mo:Ru=0.53.

total Mo, remains essentially unchanged, but Ar⁺ induced reduction of Mo(V) to Mo(IV), together with an increase in Mo(0) surface concentration after 8 min sputter etching, is clearly evident. Similar extended etching (8, 12 min) of MoO₃ alone also led to the detection of Mo(IV), but without evidence of Mo(V).^[6] With increasing Mo content (Mo:Ru=0.57 and 1.51) progressively greater surface concentrations of MoO₃ are evident, as might be expected. Highest concentrations of zerovalent Mo (also present after recycling), were detected on the most active amide hydrogenation catalysts of nominally low Mo content (Mo:Ru=0.19, 0.57), a possible implication being that Ru is more effective in the retention of reduced Mo oxidation states when initial concentrations of Mo are low. Finally, it is relevant to note that neither XRD nor XPS have provided any evidence in support of RuC formation.

Results of Control Experiments using Mo(CO)₆ Alone

Further evidence in support of the role of Ru in retention of reduced oxidation states of Mo, particularly Mo(0), has been provided by the results of the following control experiments: (a) no detectable reaction occurred during treatment of DME suspensions of MoO₃ at 100 bar H₂ and 160 °C for 16 h (normally sig-

nificantly higher temperatures are generally required for the gas phase hydrogen reduction of MoO₃, e.g., the formation of Mo₄O₁₁ and Mo₂O₅ as intermediates in the reduction of MoO₃ to MoO₂ at 300 °C^[24]); (b) partial reaction of Mo(CO)₆ in DME under the standard reaction conditions yielded MoO₃ (Mo content 66.7 wt% by ICP analysis) as the only detectable product,^[6] and (c) addition of Mo powder (which is itself inactive for amide hydrogenation) to a Ru₃(CO)₁₂ precursor in a control experiment (*cf.* Table 1, entry 6) simply maintains catalytic performance that is typical of Ru alone, indicating that bulk Mo(0) is not responsible for the synergy. Thus the presence of Ru appears crucial to the stabilisation of Mo(0), introduced as Mo(CO)₆, in the active and selective catalysts for amide reduction, most probably as a consequence of reactions between the organometallic precursors during catalyst genesis.

Catalyst Model

Addition of Mo(CO)₆ to the Ru₃(CO)₁₂ catalyst precursor at Mo:Ru compositions of ≤1 clearly has a profound effect on amide conversion and product selectivity (*cf.* Table 1, entries 1 and 3), and on the ultimate Ru particle sizes of the active materials (*cf.* Table 5, entries 1 and 2). A combination of HP-FT-IR results during catalyst genesis and *ex situ* catalyst characterisation data, for the most active and selective catalysts, seem best interpreted in terms of 2–4 nm aggregates containing Ru(0) intimately associated with Mo in oxidation states ranging between (0), (IV), (V) and (VI). Substitution of minor amounts of Mo(0) in the Ru lattice would be consistent with the slight lattice expansion evident from XRD, the detection of Mo(0) by XPS and the homogeneous distribution of Ru and Mo as revealed by EDX-STEM. The chemical states of Mo would thus range from close to metallic in areas intimately associated with the surface of Ru, to increasingly higher oxidation states, finally Mo(VI), towards the exterior surfaces of the aggregates. From XPS data, at and above the threshold Mo:Ru composition of 1, the assemblies contain progressively higher surface concentrations of Mo(VI), e.g., for Mo:Ru=1.51, Mo(VI):Mo(IV)=97:3%, which presumably serve to block active sites, with

Table 6. XPS data: quantification of Ru and Mo, and relative composition of Mo oxidation states *vs.* Ar⁺ sputter etching time (Mo:Ru=0.19 catalyst).^[a]

Sputter etching time (3 keV)	Composition [at%]					
	Ru	Mo total	Mo(VI)	Mo(V)	Mo(IV)	Mo(0)
none	87.7	12.3	6.4 (51.6)	3.0 (24.2)	1.4 (11.3)	1.6 (12.9)
1 min	89.2	10.8	5.6 (52.8)	2.0 (18.9)	1.7 (16.0)	1.3 (12.3)
8 min	90.5	9.5	4.7 (51.1)	0.4 (4.3)	2.3 (25.9)	1.8 (19.6)

^[a] Atomic% distribution of Mo oxidation states in parentheses.

consequent inhibition of all amide reduction activity. Finally, under the strongly reducing reaction conditions required for amide hydrogenation, the Ru/Mo aggregates may also conceivably exist in a form of dynamic equilibrium, with reversible formation of reduced oxidation states of Mo.

Comparison with Rh/Mo Catalysts

There are both similarities and significant differences between the Ru/Mo catalysts described here and the Rh/Mo systems recently reported for CyCONH₂ reduction.^[6] Similarities include (i) the heterogeneous nature of the catalysts, (ii) reduction of CyCONH₂ to CyCH₂NH₂ in good selectivity, (iii) no requirement for addition of ammonia or amines to suppress secondary amine formation, although minor amounts of secondary amines were always evident with Rh/Mo, (iv) critical dependence of catalyst performance on Mo:Rh composition, (v) reduction under milder reaction conditions than those commonly required by, e.g., copper chromite, (vi) a significant decrease in amide conversions below a limiting temperature and pressure of 130 °C and 100 bar H₂, respectively (*cf.* 145 °C and 20 bar H₂ with Ru/Mo), and (vii) catalysts that comprise intimate mixtures of metallic Rh and amorphous Mo (with excess Mo present in the form of MoO₃). Differences include (i) the much shorter induction period required for catalyst genesis (450 min *vs.* 130 min) with Ru/Mo for optimum catalyst compositions, which is presumably a reflection of the relative (thermal) stabilities of the penultimate Ru and Rh molecular precursors to the heterogeneous catalysts, (ii) generally slightly lower primary amine selectivities and greater variation in product selectivities throughout, with (iii) secondary amine formation in particular observed to increase significantly at low pressures, (iv) good conversions maintained up to a limiting composition threshold of Mo:Rh=2, above which no primary amine was formed, with a complete switch of product distribution in favour of (CyCH₂)₂NH and CyCH₂OH, at much lower overall conversions, and neither (v) complete catalyst deactivation evident at least as far as Mo:Rh=4.5, nor (vi) evidence of the presence of Mo(0) (XPS) or Rh lattice expansion (XRD). Overall the behaviour of the Ru/Mo catalysts appears 'cleaner' and more readily rationalised than that of their Rh/Mo counterparts.

Origin of High Selectivity towards Primary Amide Reduction

The highly selective behaviour of these Ru/Mo catalysts towards reduction of a primary amide such as CyCONH₂ with, under optimum catalyst composi-

tions, no secondary or tertiary amine formation, appears unique in the history of amide hydrogenation. Consequently, the traditional requirement for the deliberate addition of excess ammonia^[2,25] to suppress the postulated imine-amine coupling reactions responsible for by-product formation (*cf.* Scheme 1) is rendered unnecessary. It is however recognised that during the formation of CyCH₂OH, the only significant by-product detected (in *ca.* 14% selectivity) over these Ru/Mo catalysts under optimum reaction conditions, one equivalent of NH₃ is liberated per equivalent of CyCONH₂ consumed *via* this pathway, leading to the possibility that this *in situ* generation of ammonia may be sufficient to inhibit (CyCH₂)₂NH formation. Additional factors are also likely to be important, including, e.g., (i), reduced reaction temperatures in relation to those required by copper chromite-based catalysts, and (ii), the small (2–4 nm) sizes of the well dispersed nanocomposite aggregates that may facilitate rapid, solvent-assisted, desorption of primary amine into the liquid phase immediately after formation on the catalyst surface. A further point of significance is a potential role for reduced oxidation states of Mo during amide reduction, as revealed by a consideration of reports of the MoO₂-catalysed isomerisation of alkanes.^[26] Here the existence of MoO₃ and Mo₂O₅ on the surface of MoO₂ (*cf.* Figure 10) was demonstrated and considered to be the origin of both metallic and acidic functions that were responsible for unusual activity associated with this 'bifunctional' material. Analogous behaviour could equally well be of relevance to amide reduction, with the acidic function responsible for enhancement of strong initial adsorption of the amide carbonyl group, leading to synergistic hydrogen reduction at the Ru/Mo interface, with a consequent enhancement of overall conversion, as observed experimentally. An additional consequence of the acidic function may be protonation of CyCH₂NH₂ immediately on formation, leading to suppression of secondary reactions.

Conclusions

A family of recyclable heterogeneous Ru/Mo catalysts, derived from zerovalent metal carbonyls Ru₃(CO)₁₂ and Mo(CO)₆, have proved effective for the selective hydrogenation of a range of amides to the corresponding amines under significantly milder reaction conditions than those reported previously for these difficult transformations. They are particularly useful for the highly selective reduction of primary amides such as CyCONH₂ to CyCH₂NH₂, without the need for the co-addition of excess ammonia and/or amines to inhibit side reactions leading to secondary product formation, hitherto a universal feature of both amide and nitrile functional group reduction.

These catalysts have been shown to be effective for amide reduction at pressures as low as 20 bar H_2 , but the current limiting effective operational minimum temperature of 145 °C represents a further obstacle to be surmounted if they are to become attractive for the production of intermediates in the manufacture of fine chemicals and pharmaceuticals. A key factor associated with the performance of these Ru/Mo catalysts is clearly the incorporation of a formally zerovalent Mo precursor, namely $Mo(CO)_6$. This molecule, together with CO ligand-substituted derivatives, e.g., $Mo(CO)_{6-n}L_n$ ($n=1-3$; $L=N, O, P$ donor ligands, and unsaturated hydrocarbons such as arenes, dienes and trienes, e.g., bicyclohepta-2,5-diene and 1,3,5-cycloheptatriene), comprise a group of organometallic $Mo(0)$ complexes, of wide ranging stability with respect to degradation, available for catalyst tuning purposes. Application of high throughput methods, using such ligand-substituted $Mo(0)$ derivatives as precursors, may thus provide opportunities for the discovery of catalysts that are effective at lower reaction temperatures, ideally *ca.* 70 °C. Although an $Mo(0)$ catalyst precursor appears essential, this does not necessarily apply to ruthenium, as the Ru(III) complex $[Ru(acac)_3]$ has also been shown to be an acceptable precursor (cf. Table 1, entries 3 and 4), thus allowing scope for the use of more readily available Ru sources than $Ru_3(CO)_{12}$.

Our previous paper reported preliminary attempts, using silica as a 'neutral' support, to prepare, characterise and evaluate supported Rh/Mo amide reduction catalysts.^[6] Although these proved to be initially more active than their unsupported counterparts towards the reduction of *N*-acetylpiperidine, they performed poorly at <150 °C and progressively deactivated during recycle, as a consequence of accumulation of C-, H-, and N-containing residues on the support. The poor performance with respect to reduced temperatures using fresh catalysts was attributed to temperature-dependent limitations to substrate adsorption/product desorption onto/from the catalyst surface (or possibly, in light of this work, strong amide chemisorption and even oligomerisation on the silica support). Equivalent Ru/Mo catalysts have not therefore been examined. Nevertheless carbon, a standard support commonly used for metal-catalysed reductions of organic molecules may, particularly in the high surface area form, actually be more appropriate than silica, and certainly merits future consideration.

In the broader context, the approach described in this and our previous paper^[6] may also lead to the discovery and development of catalysts for the reduction of other 'difficult' organic carbonyl-containing functional groups, e.g., carboxylic acids, esters and anhydrides, the majority of which still rely on stoichiometric hydridic reagents, e.g., $LiAlH_4$ and derivatives, rather than intrinsically more efficient catalytic routes using molecular hydrogen.

Experimental Section

With the exception of the additional details provided below, experimental and analytical procedures are as outlined in ref.^[6]

Safety warning. Experiments involving pressurised gasses can clearly be hazardous and must be conducted with suitable equipment following appropriate safety procedures.

Reagents

Molybdenum hexacarbonyl, $Mo(CO)_6$, was supplied by Alfa Organics, $RuCl_3 \cdot xH_2O$ (99.9%) by Strem, Mo powder (99.8%) by Newmet, 5 wt% Ru on carbon by Aldrich Chemicals, and $Ru(acac)_3$ by Johnson Matthey. Triruthenium dodecacarbonyl, $Ru_3(CO)_{12}$, was prepared from $RuCl_3$ hydrate by the method of Johnson et al.^[27] Except where indicated otherwise the amide substrates, potential amine products and GC standards (98–99% purity) were obtained from Aldrich Chemicals. *N*-Ethylpiperidine (99%), piperidine (99%), methylcyclohexane (99%) and cyclohexanecarboxylic acid (97%) were obtained from Lancaster, and benzylamine (99%) from Acros Organics.

N,N-Dimethylcyclohexanecarboxamide, CyCON(CH₃)₂

White crystals of the title compound were prepared by hydrogenation of *N,N*-dimethylbenzamide over Pd/C (0.5 mol%) at 160 °C for 16 h; yield: 87%; mp 84–87 °C; anal. calcd. $C_9H_{17}NO$: C 69.63, H 11.04, N 9.02; found: C 68.82, H 10.95, N 8.48; ¹H NMR (200 MHz, $CDCl_3$): δ = 1.15–1.75 (m, 10), 2.43 (tt, 1), 2.86 (s, 3), 2.98 (s, 3); CI-MS: m/z = 156 $[M]^+$.

Catalytic Procedures

A typical 'single-pot' Ru/Mo catalyst preparation, and evaluation in CyCONH₂ reduction, was carried out as follows, using a nominal Mo:Ru atomic composition of 0.50. $[Ru_3(CO)_{12}]$ (0.022 g, 0.103 mmol Ru), freshly sublimed $Mo(CO)_6$ (0.0135 g, 0.0511 mmol Mo) and cyclohexanecarboxamide (0.235 g, 1.85 mmol) contained in a glass liner were dissolved in 1,2-dimethoxyethane (DME) (30 mL), affording a yellow solution [see Supporting Information, Figure S1(a)]; *n*-octane (0.100 g) was added as internal standard for GC analysis. The liner was placed in a *ca.* 300 mL capacity pressure vessel, origin of manufacture ICI, and the reaction mixture, under agitation, purged 3 times with N_2 (to 5 bar), and 3 times with H_2 (5 bar). The autoclave was then pressurised to 100 bar H_2 and heated to 160 °C for 16 h. After cooling to room temperature, the autoclave was vented and opened, revealing a very dark coloured liquid [see Supporting Information Figure S1(b)] from which a black residue slowly settled, leaving a colourless solution [see Supporting Information, Figure S1(c)]. The residue was separated by centrifugation (2000 rpm, 20 min) and the supernatant liquid containing reaction products removed. After several washings with DME (10 mL) the catalyst residue (*ca.* 15 mg) was dried, and the resultant fine black powder either recycled using the same quantities of fresh substrate and solvent, or characterised using the techniques

described below. Product solutions were analysed by GC as previously described.^[6]

Preparation of Ru/MoO₃ from Ru₃(CO)₁₂ and MoO₃

This material was obtained using the procedure described above, with [Ru₃(CO)₁₂] (0.022 g) and a suspension of the requisite amount of MoO₃ (0.0075 g) to afford a Mo:Ru composition of *ca.* 0.5, in a DME (30 mL) solution containing CyCONH₂ (0.235 g).

Ex situ Characterisation

XRD: A monochromated Co K ($\lambda = 1.7902 \text{ \AA}$) X-ray source was used.

XPS: Representative examples of both freshly prepared, and used, catalysts, together with a series of primary standards (Mo foil, MoO₃, Ru pellet and Ru powder) were analysed using a Scienta ESCA 300 XPS spectrometer at NCESS, Daresbury. The curve fitting procedure for the Mo 3d spectra involved fixing the areas of the Mo 3d_{5/2} and 3d_{3/2} lines at the theoretical ratio of 60:40, and using a ΔE value of 3.2 eV in accordance with the known separation of the 3d doublet in Mo and MoO₃.^[28,29]

EDX-STEM: Elemental compositions of the metallic components were measured using the most intense Ru and Mo L 1 α lines at 2.559 and 2.293 keV, respectively; Ru, Mo and O K 1 α lines at 19.279, 17.479 and 0.529 keV, respectively, were also used for Ru/MoO₃ sample.

Microanalysis: The term 'nominal composition' used in the text refers to the relative quantities of Ru and Mo used in the initial catalyst preparations. Unfortunately, despite numerous attempts, it proved impossible to confirm the actual compositions in the catalytically active materials by ICP-AES analysis, principally because of the well known intractable nature of Ru towards acid digestion.^[30]

Acknowledgements

The authors acknowledge the assistance of Mr. S. Apter and Mr. A. Mills for microanalyses and mass spectrometry, respectively, Dr. J. Claridge and Dr. J. A. Iggo (Department of Chemistry) and Mr. A. J. Pettman (Pfizer Ltd) for discussions, EPSRC for financial support of NCESS, Daresbury, under grant GR/S14252/01, and the Leverhulme Fine Chemicals Forum for financial support (to CP and AMS).

References

- [1] P. N. Rylander, *Hydrogenation Methods*, Academic Press, **1985**, and references therein.
- [2] B. Wojcik, H. Adkins, *J. Am. Chem. Soc.* **1934**, *56*, 247; 2419–2424.
- [3] D.-H. He, N. Wasaka, T. Fuchikami, *Tetrahedron Lett.* **1995**, *36*, 1059–1062.
- [4] T. Fuchikami, C. Hirokawa, N. Wasaka, *Tetrahedron Lett.* **1996**, *37*, 6749–6752.
- [5] A. Behr, V. A. Brehme, *Adv. Synth. Catal.* **2002**, *344*, 525–532.
- [6] G. Beamson, A. J. Papworth, C. Philipps, A. M. Smith, R. Whyman, *J. Catal.* **2010**, *103*, 93–102.
- [7] P. Kluson, L. Cerveny, *Appl. Catal. A: Gen.* **1995**, *128*, 13–31.
- [8] J. P. Breen, R. Burch, K. Griffin, C. Hardacre, M. Hayes, X. Huang, S. D. O'Brien, *J. Catal.* **2005**, *236*, 270–281.
- [9] J. Volf, J. Pašek, in: *Catalytic Hydrogenation*, (Ed.: L. Cerveny), Elsevier Science, Amsterdam, **1986**, pp 105–145.
- [10] S. Nishimura, *Handbook of Heterogeneous Catalytic Hydrogenation for Organic Synthesis*, John Wiley and Sons, Inc., New York, **2001**, and references cited therein.
- [11] H. Sigel, R. B. Martin, *Chem. Rev.* **1982**, *82*, 385–426.
- [12] See, for example, J. Clayden, N. Greeves, S. Warren, P. Wothers, *Organic Chemistry*, Oxford University Press, **2001**.
- [13] Y. Kikugawa, S. Ikegami, S. I. Yamada, *Chem. Pharm. Bull.* **1969**, *17*, 98–104.
- [14] H.-J. Zhu, K.-T. Lu, G.-R. Sun, J.-B. He, H.-Q. Li, C. U. Pittman, Jr, *New J. Chem.* **2003**, *27*, 409–413.
- [15] F. Piacenti, M. Bianchi, P. Frediani, E. Benedetti, *Inorg. Chem.* **1971**, *10*, 2759–2763.
- [16] J. W. Koepke, J. R. Johnson, S. A. R. Knox, H. D. Kaesz, *J. Am. Chem. Soc.* **1975**, *97*, 3947–3952.
- [17] H. W. Walker, C. T. Kresge, P. C. Ford, R. G. Pearson, *J. Am. Chem. Soc.* **1979**, *101*, 7428–7429.
- [18] R. Whyman, A. P. Wright, J. A. Iggo, B. T. Heaton, *J. Chem. Soc. Dalton Trans.* **2002**, 771–777.
- [19] F. A. Cotton, A. K. Fischer, G. Wilkinson, *J. Am. Chem. Soc.* **1959**, *81*, 800–803.
- [20] R. Koelliker, G. Bor, *J. Organomet. Chem.* **1991**, *417*, 439–451.
- [21] I. W. Stolz, G. R. Dobson, R. K. Sheline, *Inorg. Chem.* **1963**, *2*, 322–326.
- [22] H. E. Swanson, R. K. Fuyat, G. M. Ugrinic, *Natl. Bur. Stand. (U.S.)* **1955**, Circ. 539, Vol. IV.
- [23] A. V. Ruban, H. L. Skriver, J. S. Norskov, *Phys. Rev. B* **1999**, *59*, 15990–16000.
- [24] R. Burch, *J. Chem. Soc. Faraday Trans. 1* **1978**, *74*, 2982–2990.
- [25] A. A. N. Magro, G. R. Eastham, D. J. Cole-Hamilton, *Chem. Commun.* **2007**, 3154–3156.
- [26] A. Katrib, J. W. Sobczak, M. Krawczyk, L. Zommer, A. Benadda, A. Jablonski, G. Maire, *Surf. Interface Anal.* **2002**, *34*, 225–229.
- [27] C. R. Eady, P. F. Jackson, B. F. G. Johnson, J. Lewis, M. C. Malatesta, *J. Chem. Soc. Dalton Trans.* **1980**, 383–389.
- [28] C. D. Wagner, W. M. Riggs, L. E. Davis, J. F. Moulder, G. E. Muilenberg, *Handbook of X-ray Photoelectron Spectroscopy*, Perkin-Elmer Corporation, Physical Electronics Division, Eden Prairie, Minn. 55344, USA, **1979**.
- [29] D. Briggs, M. P. Seah, *Practical Surface Analysis*, Vol. 1, *Auger and X-ray Photoelectron Spectroscopy*, 2nd edn., Wiley, New York, **1990**, and references cited therein.
- [30] M. Balcerzak, *Crit. Rev. Anal. Chem.* **2002**, *32*, 181–226.